Journal of Pharmaceutical Sciences xxx (2017) 1-5

Contents lists available at ScienceDirect

Journal of Pharmaceutical Sciences

journal homepage: www.jpharmsci.org

Pharmaceutics, Drug Delivery and Pharmaceutical Technology

A Study of Fasoracetam's Solid State Forms: A Potential Anti-Alzheimer Pharmaceutical

Bram Harmsen [1], Koen Robeyns [1], Johan Wouters [2], Tom Leyssens [1,*]

[1] Institute of Condensed Matter and Nanosciences, Université Catholique de Louvain, Louvain-la-Neuve, Belgium
[2] Namur Institute for Life Sciences (Narilis), University of Namur, Namur, Belgium

ARTICLE INFO

Article history:
Received 21 September 2016
Revised 21 December 2016
Accepted 11 January 2017

Keywords:
polymorphism
crystal structure
thermogravimetric analysis
calorimetry (DSC)
solvent evaporation
hydrate
Alzheimer's disease

ABSTRACT

Different solid state forms of the research chemical fasoracetam, which counters the effects of Alzheimer's disease, have been subjected to a thermal and structural analysis. Single crystals were obtained from solution evaporation and from the melt. Single-crystal X-ray analyses of the crystals show the existence of 2 hydrated and 1 non-hydrated crystalline form of fasoracetam. Under ambient conditions, the hydrate form I is found to be the most stable form, showing a melting point of 57C. This low melting point, combined with possible water losses could cause problems when formulating the hydrated form and impact the storage conditions of the compound.

Introduction

Fasoracetam (NS-105, 5-oxo-D-prolinepiperidinamide) is part of the racetam family, a drug of the pyrrolidone class and currently considered a research chemical.[1] The class is characterized by its nootropic (e.g., piracetam and fasoracetam), stimulating (e.g., oxiracetam), and anticonvulsant (e.g., levetiracetam) properties.[2-6] Studies have shown promising results in its ability to counter and reverse the effect of Alzheimer's disease.[7-9] It is a known fact that the nature of a solid state form directly impacts bioavailability,[10,11] solubility[12,13] and other pharmacokinetic parameters, which need to be controlled for maximum dosage effect and consistency. It is therefore important to exercise control over the solid phase form.[14,15] Screening for different solid phases of novel drugs has now become an integral part of the drug development process.[16,17] Additionally, legal instances still consider alternative solid forms as novel, hence a formulation with such a novel form would not infringe an existing patent.[18] Besides identifying different solid forms, an understanding of the thermodynamic relationships between these forms is also recommended, to avoid future issues related to phase transformations, as illustrated by the Ritonavir and Rotigotine cases, where a market withdrawal of the drug occurred due to phase transformations of the active pharmaceutical ingredient.[19,20]

Fasoracetam (Scheme 1) is a promising research chemical and is available in solid form at ambient conditions. However, no crystal structure has yet been reported in the literature, nor any solid screen performed for this compound. The chemical structure of fasoracetam shows 2 amide functions which commonly take part in hydrogen bonding patterns, as the carbonyl can serve as a hydrogen acceptor, whereas the amide can act as a hydrogen donor. Having multiple hydrogen bonding sites available, this could possibly lead to different packing arrangements. Furthermore, other racetam compounds have already shown a propensity toward the formation of multiple solid state forms.[21]

In this contribution, we therefore set out to identify different solid state forms of fasoracetam and describe these from a structural as well as a thermodynamical point of view. We identified a stable hydrated form (hydrate I), but also a second polymorphic form of the hydrate (hydrate II). Using specific conditions, an anhydrated form could also be isolated. All forms are structurally described and a full thermodynamic analysis on all forms was performed.

This article contains supplementary material available from the authors by request or via the Internet at http://dx.doi.org/10.1016/j.xphs.2017.01.016.

* *Correspondence to:* Tom Leyssens (Telephone: +32-10-47-28-11; Fax: +32-10-47-27-07).
E-mail address: Tom.Leyssens@uclouvain.be (T. Leyssens).

http://dx.doi.org/10.1016/j.xphs.2017.01.016
0022-3549/

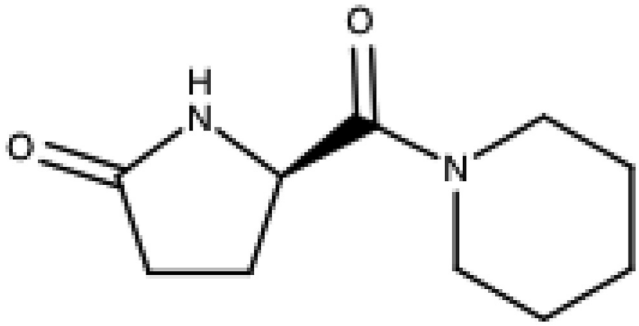

Scheme 1. Chemical structure of fasoracetam.

Materials and Methods

Materials

Fasoracetam was ordered from Jinan HaoHua Industry Co., Ltd., and used as received. It was identified via X-ray powder diffraction to be the most stable form of the hydrate (hydrate I).

All solvents used were obtained from VWR International S.A.S. and used without further purification.

Methods

Single-crystal x-ray diffraction (SC-XRD) experiments were collected on a mar345 image plate using MoKα radiation (Rigaku Ultra X18S generator, Fox3D mirrors). Crystals were picked up using a little grease, and for low temperature experiments (Table 2) the crystal was flash frozen in an N_2 flow prior to data collection. Data images were integrated by CrysAlisPRO[22] and the implemented multi-scan absorption correction was applied. All structures were solved by SHELXS-97 and refined by SHELXL-2014/7.[23] All non-hydrogen atoms were refined anisotropically and H-atoms were placed on calculated positions with isotropic temperature factors 1.2 times Ueq of their parent atoms. For the anhydrate structure, the piperidine rings were found to be disordered with the minor fraction <10%. The minor part was restrained to be similar (bond and angles) to the main fraction. Molecular structures were created using mercury.[24]

Powder x-ray diffraction (XRPD) measurements were performed on a Siemens D5000 diffractometer equipped with a Cu X-ray source operating at 40 kV and 40 mA. A secondary monochromator allowed the selection of Kα radiation of Cu ($\lambda = 1.5418$ Å). A scanning range of 2θ values from 2 to 72 at a scan rate of 0.6/min was applied.

Differential scanning calorimetry (DSC) measurements were performed on a Mettler Toledo DSC821^e using 40 μL aluminum crucibles without pin, with the method increasing from 25C to 250C with a step size of 10C/min under continuous nitrogen flow. The method used to determine the melting points can be found in Supplementary Information, Section 3.

Thermogravimetric analysis (TGA) measurements were performed on a Mettler Toledo TGA/SDTA851^e using an aluminum crucible, with the method increasing from 25C to 350C with a step size of 10C/min while maintaining a nitrogen flow of 50.0 mL/min.

Single Crystal Growth and Form Screening

The single crystals obtained for SC-XRD analysis were grown via different methods. Initially, fasoracetam (as received, hydrate form I) was recrystallized from water using solvent evaporation. The second hydrate, form II, is less stable and was obtained from methanol evaporation, which provided large enough single crystals. The anhydrate form could not be crystallized from any of the solvents used. To obtain this form, a recrystallization from the melt was performed *in vacuo*, where it was kept at 60C for 1 week. These conditions allowed water to be removed from the melt. After a 1-week period the temperature was lowered while maintaining vacuum conditions, which resulted in a different solid form, the anhydrate, with crystals suitable for SC-XRD analysis. Starting from hydrates I and II, both convert into the same anhydrated form using the method described above.

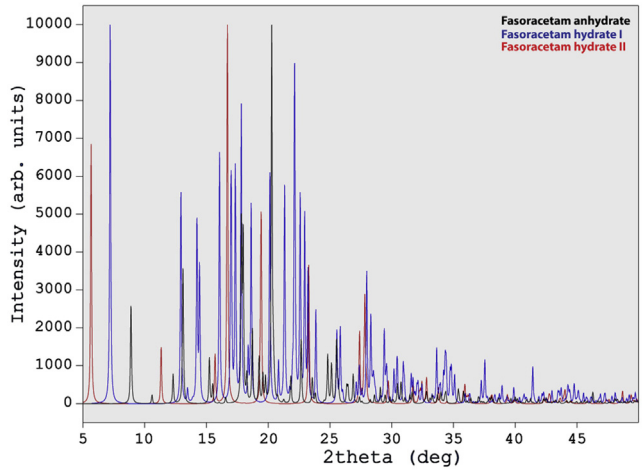

Figure 1. Fasoracetam powder patterns simulated from SC-XRD.

In this contribution, we also present a solid form screen of fasoracetam. Even though the screen is limited, 3 different forms of fasoracetam have been identified. Initially, a first screen was performed based on the solvent evaporation principle. The purchased compound was dissolved in the solvents investigated and the solution was left to evaporate completely.

Results and Discussion

Form Screening

Once the solution was evaporated completely, the powders obtained from the solvent screen were directly analyzed using XRPD (experimental patterns can be found in Supplementary Information, Section 1). The different solid state forms obtained are shown in Figure 1 and it was later confirmed that 2 forms are polymorphically related (hydrate I and II, respectively), which are both a 1:1 hydrated form. The results obtained are shown in Table 1.

Solvent evaporation does not lead to the formation of an anhydrate form, but instead 2 different hydrates were found via XRPD. The hydrate form obtained from each solvent appears to be random, as no correlation among evaporation rate, hygroscopicity, and polarity can be found.[25,26] Crystals obtained by water and methanol evaporation were found suitable for SC-XRD analysis, which showed a 1:1 stoichiometric hydrate form in both cases, named hydrate I and hydrate II, respectively. As will be shown later, hydrate I has a melting point at 57C and hydrate II has a melting point at about 48C.

A structural analysis of all hydrogen bonding patterns is given below, followed by a thermal analysis.

Structural Analysis

Figure 2 shows the hydrogen bonding pattern for the anhydrate phase. This bonding network corresponds to an $\boldsymbol{R_2^2(9)}$ synthon (Etter's graph set notation[27]), composed of a N-H group of the

Table 1
Solvent-based Solid Form Screen for Fasoracetam

Solvent	Crystal Form (XPRD)
Water	Hydrate I
Acetonitrile	Hydrate II
Methanol	Hydrate II
Ethyl acetate	Hydrate I
Acetone	Hydrate I
Dichloromethane	Hydrate II
Tetrahydrofuran	Hydrate I
Chloroform	Hydrate II
Toluene	Hydrate II

XPRD, x-ray powder diffraction.

pyrrolidone ring of the first molecule forming a hydrogen bond with the pyrrolidone carbonyl of a second molecule. A second hydrogen bond links the bridging carbonyl of the first molecule to the N-H group in the pyrrolidone ring of the second molecule. This hydrogen bonding pattern is the only pattern present in the crystal structure.

The hydrate form I of fasoracetam (Fig. 3) is a stoichiometric hydrate with one water molecule per fasoracetam molecule. The high number of hydrogen donors and acceptors present create a complex hydrogen bonding network. The water molecules serve as bridge between fasoracetam molecules with both hydrogens forming a bond with a carbonyl group of 2 different pyrrolidone rings. A second hydrogen bond from the N-H group on the first pyrrolidone ring to the carbonyl on the second leads to a closed-ring $\boldsymbol{R_3^2(8)}$ pattern, which can be seen in the center-bottom of Figure 3.

As shown in Figure 3, it is important to note that the water molecule functioning as a double donor lies flat in the plane with both pyrrolidone moieties of the fasoracetam molecules. This interaction, as described above, creates a ring-like arrangement of water and fasoracetam molecules all within the same plane as emphasized by the ball and stick representation. Interestingly, the water molecule serving as a double hydrogen donor in the ring arrangement also acts as an acceptor for a second water molecule, having a proton lying perpendicular to the aforementioned plane. This hydrogen bond connects the different ring-like arrangements in a step-like pattern from an extended point of view. The hydrogen bonds described here can be described as $\boldsymbol{D_3^3(6)}$. Therefore, the water molecules can also be seen as molecules that connect different planes.

In Figure 4, the hydrogen bonding pattern of the hydrate form II is shown. The main difference between this and the previous

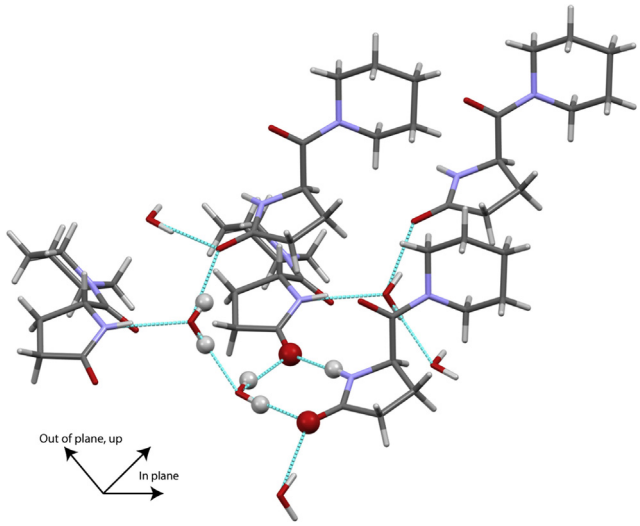

Figure 3. Hydrogen bonding pattern of hydrate I.

hydrate form is the location of the water molecules. All hydrogen bonds lie within the same plane, forming a sheet. Contrary to hydrate form I, there are no hydrogen bonds out of the plane, linking the sheets together. Additionally, where in hydrate form I fasoracetam molecules directly form hydrogen bonds with each other, this is not observed in hydrate form II and all hydrogen bonds go via water molecules. Sheets are therefore held together by interactions other than hydrogen bonding ones, which will likely explain why this hydrate form is less stable, as shown later on. Each water molecule serves as a double hydrogen donor, forming hydrogen bonds with the pyrrolidone carbonyl groups of 2 distinct fasoracetam molecules. Simultaneously, the same water molecule also acts as an acceptor, forming a hydrogen bond with the pyrrolidone N-H group of a third fasoracetam molecule. These interactions connect the whole sheet together and can be described as $\boldsymbol{R_4^3(10)}$. The crystal structure data of the 3 forms can be found in Table 2.

As shown by this table, when the Z value for hydrate II is adjusted to one formula unit its volume becomes 286.74 Å^3. This is slightly bigger than the volume taken by hydrate form I, 282.96 Å^3. It seems that the reorientation of one of the water molecules for hydrate I results in a slightly more compressed structure as a whole, which could yield stronger (shorter) hydrogen bonds or the formation of new hydrogen bonds due to the molecules' closer proximity. However, because the data have been collected at different temperatures (150 K for hydrate II and 297 K for hydrate I), the

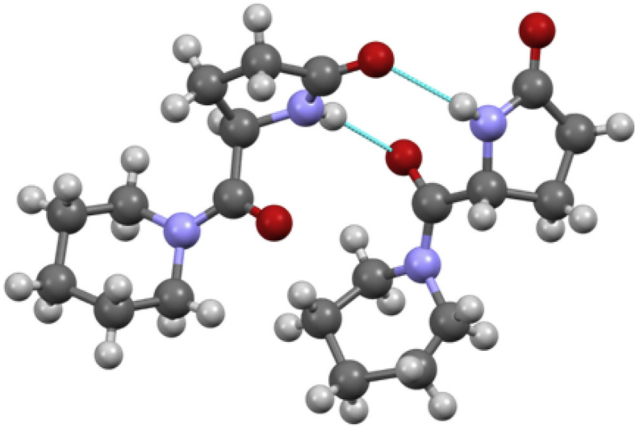

Figure 2. Fasoracetam anhydrate hydrogen bonding pattern.

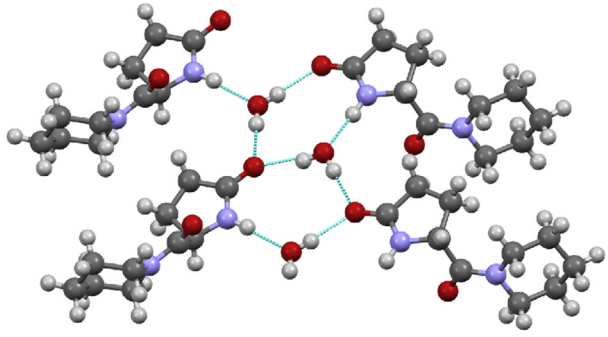

Figure 4. Fasoracetam hydrate II hydrogen bonding pattern.

Table 2
Crystal Structure Data of All Fasoracetam Forms

Variable	Fasoracetam Hydrate I	Fasoracetam Hydrate II	Fasoracetam Anhydrate
Cambridge Crystallographic Data Center number	1489556	1489557	1489558
Chemical formula	$C_{10}H_{16}N_2O_2 \cdot H_2O$	$C_{10}H_{16}N_2O_2 \cdot H_2O$	$C_{10}H_{16}N_2O_2$
M_r	214.26	214.26	196.25
Crystal system, space group	Triclinic, P1	Monoclinic, C2	Orthorhombic, $P2_12_12_1$
Temperature (K)	297	150	297
a, b, c (Å)	6.6093 (7), 7.0801 (7), 12.7221 (18)	11.2982 (6), 6.5055 (4), 15.6050 (10)	9.2095 (5), 11.5104 (8), 19.7276 (13)
α, β, γ (°)	99.691 (10), 100.272 (10), 99.363 (9)	90, 90.291 (5), 90	90, 90, 90
V (Å^3)	565.91 (12)	1146.96	2091.2 (2)
Z	2	4	8
Radiation type	MoKα	MoKα	MoKα
μ (/mm)	0.09	0.09	0.09
Crystal size (mm)	0.21 × 0.11 × 0.05	0.30 × 0.05 × 0.03	0.5 × 0.4 × 0.4
T_{min}, T_{max}	0.755, 1.000	0.944, 1.000	0.423, 1.000
No. of measured, independent, observed [$I > 2\sigma(I)$] reflections	7583, 4076, 3401	4481, 2027, 1737	8790, 3731, 3160
R_{int}	0.051	0.032	0.034
θ_{max}	25.525	25.179	25.206
R [$F^2 > 2\sigma(F^2)$], $wR(F^2)$, S	0.046, 0.122, 1.05	0.041, 0.097, 1.06	0.044, 0.122, 1.02
No. of parameters	277	143	308
No. of restraints	3	1	12
$\Delta\rho_{max}$, $\Delta\rho_{min}$ (e/Å^3)	0.13, −0.12	0.18, −0.14	0.13, −0.13

difference is likely negligible. When both hydrate forms are compared for the number and composition of hydrogen bonds, the increased stability for hydrate I becomes apparent. Hydrate form II has a total of 5 unique hydrogen bonds, all of them with water molecules. The more stable form, hydrate I, has 10 unique hydrogen bonds and these are made up of hydrogen bonds with water molecules like in hydrate II, but hydrogen bonds directly between fasoracetam molecules are also present. The increased amount of unique hydrogen bonds together with different hydrogen bond types is the likely reason for the higher stability of hydrate form I.

Thermal Analysis

A thermal analysis of all forms was performed in order to characterize the fasoracetam forms and to identify the stability of different forms. TGA measurements (Fig. 5) clearly mark the difference between the hydrated and anhydrated form. The anhydrate (red line) clearly shows no particular weight loss up until degradation, which occurs at around 260C. The fasoracetam hydrate I (blue line), on the other hand, shows a first onset of weight loss at 41C. The weight loss continues up to 185C. When the temperature is increased further, degradation occurs, starting around 260C. The initial loss corresponds to 1.1 equivalent of water, as expected for a 1:1 stoichiometric hydrate. The slight deviation from the ideal stoichiometric ratio can be attributed to the crystallization conditions (the bulk material was obtained from an aqueous solution and the water remaining on the crystal surface or trapped between crystals is likely to cause the deviation observed). The fasoracetam hydrate II (green line) also shows a first onset of weight loss at 41C and continues up to 183C. Analogous to hydrate I, degradation occurs which starts around 268C. The observed water loss here is 0.9 equivalent, which is expected for a stoichiometric hydrate.

The DSC measurements (Fig. 6) show clear single melting events for all forms, as depicted by the sharp endothermic peaks. In the case of fasoracetam hydrate II (green line), the onset of the melting point was determined at 47.8C. For fasoracetam

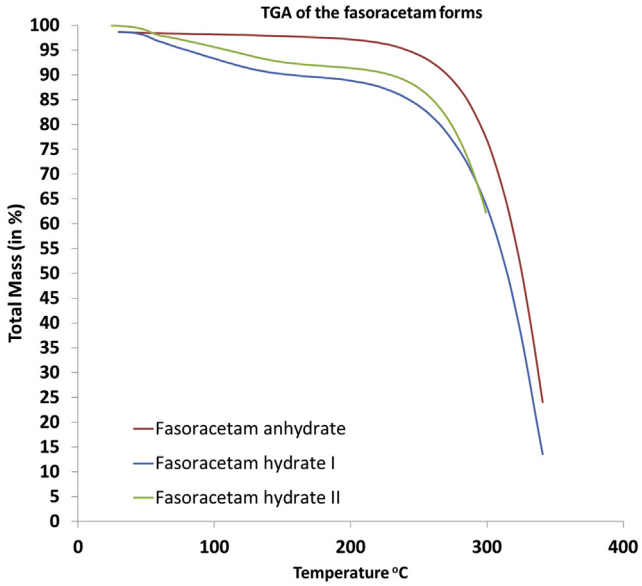

Figure 5. TGA of fasoracetam hydrates and anhydrate.

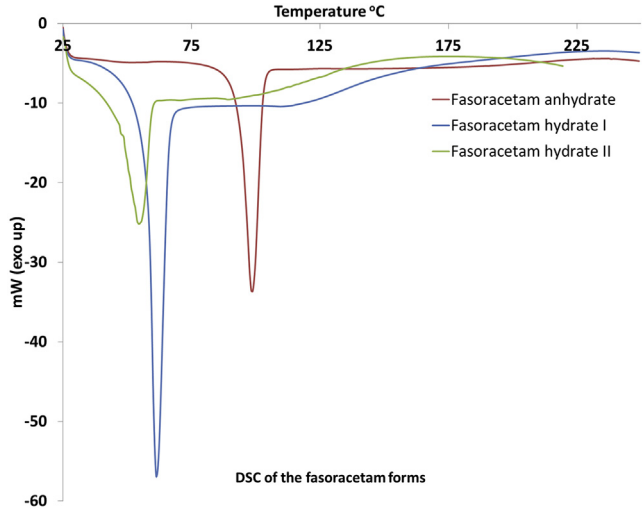

Figure 6. DSC of fasoracetam hydrates I and II, and the anhydrate.

Table 3
Enthalpies of Fusion for Fasoracetam Forms

Enthalpy of Fusion (ΔH_{fus}, J/g)		
Fasoracetam hydrate I	Fasoracetam hydrate II	Fasoracetam anhydrate
−120.9 J/g	−79.0 J/g	−76.7 J/g

hydrate I (blue line), the onset of the melting point was determined at 57.2C. This explains that the expected loss in mass starting at 41C (TGA measurement) is likely due to surface water. The continuation of mass loss occurs upon melting of the sample. The continued energy input (extended shoulder following the melting peak) after melting suggests that water is evaporating. This finding is supported by the other hydrate, form II, which exhibits the same behavior. The evaporation continues up until around 185C, which is in agreement with the data obtained from the TGA. The melting points of hydrates I and II occur prior to the water loss. This indicates that water is lost after melting and one is not dealing with dehydration of the hydrate to yield an amorphous or other anhydrous crystalline form. This is furthermore confirmed visually (see Supplementary Information, Section 2) when the sample is heated to 60C. As expected, the anhydrate form (red line) shows a single melting point, with an onset at 92.6C. The relatively small difference in melting points between the 2 hydrated forms could suggest that a solid-solid phase transformation can occur. Taking the structural data into account, it would most likely consist of a transformation from a two-dimensional sheet-like hydrogen bonding network (hydrate II) to a three-dimensional connected sheets hydrogen bonding network. The large difference in melting points between the hydrates and the anhydrate form suggests that conversion of the hydrates into the anhydrate is unlikely at ambient conditions. Investigation of the anhydrate shows that conversion to the stable hydrate occurs at ambient conditions over a 1-week period (the conversion was tracked on a daily basis via XRPD).

Using Burger's Heat of Fusion rule[28] for both hydrated forms (Table 3), they should be monotropically related. Because both hydrates were obtained from different solvents (water and methanol for hydrates I and II, respectively), a slurrying experiment where both vials were seeded with the opposite hydrate was performed and left under these conditions for 1 week. After analyzing both vials with XRPD, it turned out that both contained hydrate form I suggesting complete solution mediated polymorphic transition from form II to form I. Therefore, we can conclude that hydrate II is the less stable hydrate.

Conclusion

The research chemical fasoracetam has been subjected to a solvent screen, followed by thermal and structural analysis. Three solid forms have been successfully identified. SC-XRD shows 2 hydrated and 1 anhydrated solid form. TGA and DSC data confirm the existence of the 3 fasoracetam forms. Initial results seem to indicate the possibility to formulate both hydrate I and anhydrate forms in future pharmacological applications. However, the melting point of hydrate form I (57.2C) might be too low, where potential varying (storage) conditions might limit shelf-life or a consistent drug dosage of the anhydrate form.

Acknowledgments

This work was supported by Université Catholique de Louvain and Fonds National de Recherche Scientifique (Projet de Recherche T009913F). B.H. has recently received an Fonds dde Recherche Industrielle et Agricole grant (FC 02573).

References

1. Shorvon S. Pyrrolidone derivatives. *Lancet*. 2001;358(9296):1885-1892.
2. Löscher W, Richter A. Piracetam and levetiracetam, two pyrrolidone derivatives, exert antidystonic activity in a hamster model of paroxysmal dystonia. *Eur J Pharmacol*. 2000;391(3):251-254.
3. Waegemans T, Wilsher CR, Danniau A, Ferris SH, Kurz A, Winblad B. Clinical efficacy of piracetam in cognitive impairment: a meta-analysis. *Dement Geriatr Cogn Disord*. 2002;13(4):217-224.
4. Winblad B. Piracetam: a review of pharmacological properties and clinical uses. *CNS Drug Rev*. 2005;11(2):169-182.
5. Perucca E, Parini J, Albrici A, Visconti M, Ferrero E. Oxiracetam pharmacokinetics following single and multiple dose administration in the elderly. *Eur J Drug Metab Pharmacokinet*. 1987;12(2):145-148.
6. Gambardella A, Labate A, Colosimo E, Ambrosio R, Quattrone A. Monotherapy for partial epilepsy: focus on levetiracetam. *Neuropsychiatr Dis Treat*. 2008;4(1):33-38.
7. Gualtieri F, Manetti D, Romanelli MN, Ghelardini C. Design and study of piracetam-like nootropics, controversial members of the problematic class of cognition-enhancing drugs. *Curr Pharm Des*. 2002;8(2):125-138.
8. Gualtieri F, Guandalini L, Manetti D, Martini E, Romanelli M. Cognition-enhancing drugs in mild cognitive impairment (MCI) and Alzheimers disease (AD): an update [1]. *Med Chem Rev*. 2005;2(6):471-487.
9. Mukai H, Sugimoto T, Ago M, et al. Pharmacokinetics of NS-105, a novel cognition enhancer. 2nd communication: distribution and transfer into fetus and milk after single administration, and effects of repeated administration on pharmacokinetics and hepatic drug-metabolizing enzyme activities in rats. *Arzneimittelforschung*. 1999;49(12):977-985.
10. Enna SJ, Bylund DB. xPharm: the comprehensive pharmacology reference. Available at: http://www.sciencedirect.com/science/referenceworks/9780080552323. Accessed February 3, 2017.
11. Paixão P, Gouveia LF, Morais JAG. Prediction of the human oral bioavailability by using in vitro and in silico drug related parameters in a physiologically based absorption model. *Int J Pharm*. 2012;429(1-2):84-98.
12. Li Z, Lee PI. Investigation on drug solubility enhancement using deep eutectic solvents and their derivatives. *Int J Pharm*. 2016;505(1-2):283-288.
13. Amidon GL, Lennernäs H, Shah VP, Crison JR. A theoretical basis for a biopharmaceutic drug classification: the correlation of in vitro drug product dissolution and in vivo bioavailability. *Pharm Res*. 1995;12(3):413-420.
14. Mukai H, Sugimoto T, Ago M, Morino A. Pharmacokinetics of NS-105, a novel cognition enhancer. *Arzneimittelforschung*. 2011;49(11):881-890.
15. Ogasawara T, Itoh Y, Tamura M, et al. Involvement of cholinergic and GABAergic systems in the reversal of memory disruption by NS-105, a cognition enhancer. *Pharmacol Biochem Behav*. 1999;64(1):41-52.
16. Dai WG, Pollock-Dove C, Dong LC, Li S. Advanced screening assays to rapidly identify solubility-enhancing formulations: high-throughput, miniaturization and automation. *Adv Drug Deliv Rev*. 2008;60(6):657-672.
17. Campeta AM, Chekal BP, Abramov YA, et al. Development of a targeted polymorph screening approach for a complex polymorphic and highly solvating API. *J Pharm Sci*. 2010;99(9):3874-3886.
18. Blasi P, Schoubben A, Giovagnoli S, Rossi C, Ricci M. Fighting tuberculosis: old drugs, new formulations. *Expert Opin Drug Deliv*. 2009;6(9):977-993.
19. Morissette SL, Soukasene S, Levinson D, Cima MJ, Almarsson O. Elucidation of crystal form diversity of the HIV protease inhibitor ritonavir by high-throughput crystallization. *Proc Natl Acad Sci U S A*. 2003;100(5):2180-2184.
20. Rietveld IB, Céolin R. Rotigotine: unexpected polymorphism with predictable overall monotropic behavior. *J Pharm Sci*. 2015;104(12):4117-4122.
21. Dematos LL, Williams AC, Booth SW, Petts CR, Taylor DJ, Blagden N. Solvent influences on metastable polymorph lifetimes: real-time interconversions using energy dispersive X-ray diffractometry. *J Pharm Sci*. 2007;96(5):1069-1078.
22. Rigaku Corporation. *CrysAlis(Pro) Software System, Version 1.171.37.31*. Yarnton, England: UK Ltd.; 2014.
23. Sheldrick GM. Crystal structure refinement with SHELXL. *Acta Crystallogr C Struct Chem*. 2015;71:3-8.
24. Bruno IJ, Cole JC, Edgington PR, et al. New software for searching the Cambridge Structural Database and visualizing crystal structures. *Acta Crystallogr B*. 2002;58(3 Pt 1):389-397.
25. Comyn J. Handbook of organic solvent properties. *Int J Adhes Adhes*. 1997;17(2):177.
26. Williams DBG, Lawton M. Drying of organic solvents: quantitative evaluation of the efficiency of several desiccants. *J Org Chem*. 2010;75(24):8351-8354.
27. Etter MC, MacDonald JC, Bernstein J. Graph-set analysis of hydrogen-bond patterns in organic crystals. *Acta Cryst*. 1990;B46:256-262.
28. Burger A, Ramberger R. On the polymorphism of pharmaceuticals and other molecular crystals. I. Theory of thermodynamic rules. *Mikrochim Acta*. 1979;72(3-4):259-271.